Proceedings of the
44th IEEE Conference on Decision and Control, and
the European Control Conference 2005
Seville, Spain, December 12-15, 2005

MoB04.1

Optimal Nonlinear Control of Two-Link Flexible Arm with Adaptive Internal Model

Mustafa Doğan[1,2], Yorgo Istefanopulos[3,1]

Department of Electrical and Electronics Engineering
[1]*Boğaziçi University,* [2]*Başkent University,* [3]*Işık University, Turkey*

Abstract

The control of highly nonlinear multi-link flexible arms is subject to uncertainties caused by backlash, payload changes and external disturbances.Therefore, adaptive and robust control of multi-link flexible arms is a challenging problem.In this paper, the internal model approach is adaptively tuned up for unknown disturbances, parallel with a robust stabilizer. The stabilizer part of the controller is optimized with a new evolutionary algorithm.

I. INTRODUCTION

Two main advantages of flexible robot arms are less weight and low energy consumption. However, the structural modelling and the control design of the flexible arm are much more complicated due to nonlinear coupling between elastic and rigid modes during the complex maneuvers especially with high angular velocities. Various methods have been proposed for control of flexible-link manipulators in the literature. Hybrid control of a single flexible-link manipulator using feedback linearization and singular perturbation approach has been used in [1]. Adaptive feedback linearization has been applied successfully for a nonlinear discrete-time model of a single-link flexible manipulator [2]. Singular perturbation theory has also been used for position and force control in [3]. Strain feedback and active vibration control [4] are other approaches different from the integrated structure-control in [5]. The feedback linearizable nonlinear systems that are subject to periodic disturbances are examined either for known disturbances [6] or for unknown disturbances [7]. In [6], the known disturbances are assumed not to excite zero-dynamics. In [7], unknown disturbances included can excite high-frequency modes generated by the nonlinearities of the plant. In this research, adaptive internal model approach [7] has been modified to manage totally unknown disturbances that can include neglected higher modes of the flexible links and also large parameter uncertainties such as tip mass changes.

II. ANALYTICAL MODEL

A mathematical model of flexible-link arms can be obtained by either assumed modes [8] or finite element
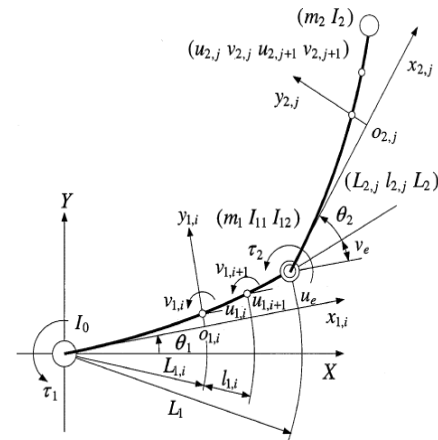

Fig. 1. Arm configuration [5]

methods [5]. Based on the results presented in [9], in this paper the finite element method has been used, since it gives more accurate results [10] and lends itself ideally to dynamic real-time controller implementations. Since the ratio between the length of the beam and its thickness is sufficiently large such that $200 \gg 10$ as proposed in [11], [12], links can be modelled as Euler-Bernoulli beams, which can only be deformed in the flexural direction. Coulomb and viscous friction are also included. The links are modelled in clamped-free configuration, since natural modes of the separated clamped-free links agree very well with actual ones compared to pinned-free configuration [13].

Referring to Figure 1, OXY: global inertial system of coordinates; $o_{1,i}x_{1,i}y_{1,i}$: body-fixed system of coordinates attached to the element i of undeformed link 1, $o_{2,i}x_{2,i}y_{2,i}$: body-fixed system of coordinates attached to the element i of undeformed link 2, L_1, L_2 total lengths of links 1 and 2, $L_{1,i}$: accumulated length of first $(i-1)$ elements of link 1, $L_{2,j}$: accumulated length of first $(j-1)$ elements of link 2, $l_{1,i}$ and $l_{2,j}$: lengths of element i of link 1 and element j of link 2, θ_1, θ_2: angular displacements of links 1 and 2, $(u_{1,i}, v_{1,i})$: flexural displacement and slope of node i of link 1, $(u_{2,j}, v_{2,j})$: flexural displacement and slope of node j of link 2,

(u_e, v_e): flexural displacement and slope at the end of link 1; I_0, I_2: moments of inertia of joint 1 and tip; I_{11}, I_{12}: moments of inertia of joint 2 rotating with links 1 and 2; m_2: tip mass; τ_1, τ_2: motor torques at joints 1 and 2, C_f: coefficient of Coulomb friction, V_f: coefficient of viscous friction [5].

A. Equations of Motion

The dynamic equations of motion can be obtained by employing the Lagrange's equations for details see [14, section 2]. Because of the high computational cost for simulating the system of equations and the complexity of the dynamic model, modal truncation is needed to select lower frequency modes of the flexible links. Since the lowest resonant frequencies of the neglected higher modes are almost tenfold of the retained first modes in the present work, and their corresponding amplitudes about $\frac{1}{100}$ of the amplitude of the first modes [15, ch. 4], therefore their contribution to the vibration can be negligible [11]. After transformation the equations of motions can be expressed as

$$\hat{M}(\hat{\mathbf{q}})\ddot{\hat{\mathbf{q}}} + \hat{C}(\hat{\mathbf{q}}, \dot{\hat{\mathbf{q}}})\dot{\hat{\mathbf{q}}} + \hat{K}\hat{\mathbf{q}} = \hat{b}\tau \qquad (1)$$

In the present work the transformation(e.g. $\hat{M} = M\varphi$) is carried automatically by the symbolic derivation program and equations of motion are obtained readily in the form suitable for analysis and simulation. For simulation and design of the controller only the first modes of both links are selected such that

$$\hat{\mathbf{q}} = \begin{pmatrix} \theta_1 - \theta_{1d} & \theta_2 - \theta_{2d} & q_3 & v_e & q_5 \end{pmatrix}^T$$

where q_3 and q_5 are the first modes of links 1 and 2, respectively, and v_e, the slope at the end of link 1, had to be retained during transformation, since it enters the equations of motion nonlinearly.

III. CONTROLLER DESIGN

A. Controller for Non-adaptive Case

The nonlinear dynamic state feedback controller is used both to damp the elastic vibrations and to reach a given end-point position. By using equation (1) and the matrix $D = \varphi^T M^{-1}$, letting $\mathbf{q} = (\hat{\mathbf{q}}^T \quad \dot{\hat{\mathbf{q}}}^T)^T$ and multiplying both sides with the inverse of the inertia matrix, we obtain the system equation with the friction

$$\dot{\mathbf{q}} = f(\mathbf{q}) + \begin{bmatrix} g_1 & g_2 \end{bmatrix} \begin{bmatrix} u_1 - V_f\dot{\theta}_1 - C_f sign(\dot{\theta}_1) \\ u_2 - V_f\dot{\theta}_2 - C_f sign(\dot{\theta}_2) \end{bmatrix}$$

$$\mathbf{y} = h(\mathbf{q})$$

where $f(0) = h(0) = 0$. Since $sign(x)$ function is non-analytical, it must be replaced by $\frac{2}{\pi}arctan(10^6 x)$ due to smoothness (differentiability) assumption of feedback linearization theory [16] and explicitly we get

$$\dot{\mathbf{q}} = \begin{bmatrix} q_6 \\ q_7 \\ q_8 \\ q_9 \\ q_{10} \\ f_6 \\ f_7 \\ f_8 \\ f_9 \\ f_{10} \end{bmatrix} + \begin{bmatrix} 0 \\ 0 \\ 0 \\ 0 \\ 0 \\ D_{11} \\ D_{21} \\ D_{31} \\ D_{41} \\ D_{51} \end{bmatrix} u_1 + \begin{bmatrix} 0 \\ 0 \\ 0 \\ 0 \\ 0 \\ D_{12} \\ D_{22} \\ D_{32} \\ D_{42} \\ D_{52} \end{bmatrix} u_2 \quad (2)$$

$$\mathbf{y} = \begin{bmatrix} 1 & 0 & 0 & 0 & 0 & 0 & 0 & 0 & 0 & 0 \\ 0 & 1 & 0 & 0 & 0 & 0 & 0 & 0 & 0 & 0 \end{bmatrix} \mathbf{q}$$

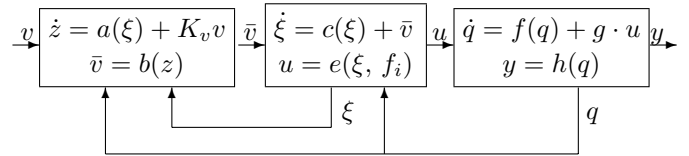where $f_i(q)$ is a nonlinear function of the modal coordinates.

Fig. 2. Dynamic State Feedback Control Scheme

In Figure 2, $a(0) = b(0) = c(0) = d(0) = e(0,0) = 0$, and $q(0) = 0_{10 \times 1}$, $z(0) = 0_{6 \times 1}$, $\xi(0) = d(z)$. Also $a, b, c, d \in \mathbf{R}^6$, and $e \in \mathbf{R}^2$ are linear vector functions in their arguments. Since the auxiliary states (z_i's) are dummy, the dimension of the closed-loop system became 16. In order to obtain a linear and controllable system from the nonlinear system (2) and to follow the steps of exact feedback linearization as defined in [16], the relative degree of the system has to be determined such that

$$\begin{aligned}
L_f h_1(\mathbf{q}) &= q_6 \\
L_f h_2(\mathbf{q}) &= q_7 \\
L_f^2 h_1(\mathbf{q}) &= f_6 \\
L_f^2 h_2(\mathbf{q}) &= f_7 \\
L_g L_f h(\mathbf{q}) &= \begin{bmatrix} D_{11} & D_{12} \\ D_{21} & D_{22} \end{bmatrix}
\end{aligned}$$

where $L_{(.)}(.)$ denotes the Lie [1] derivative. Since the modal transformation matrix Φ and inertia matrix M are nonsingular, so is D ($\forall \mathbf{q}$ including origin), the global relative degree of the system is $\{r_1, r_2\} = \{2, 2\}$ and

---
[1]The Lie derivatives are defined as follows: $L_f h(q) = \left[\frac{\partial h(q)}{\partial q}\right]^T \cdot f(q)$. The multiple Lie derivative yields: $L_f^k h(q) = \left[\frac{\partial L_f^{k-1} h(q)}{\partial q}\right]^T \cdot f(q)$

the dimension of the system (2) is $n = 10$. Since $r = 2 + 2 = 4 < 10$, dynamic state feedback can be applied. The dynamic extension algorithm [16, ch. 5] has been applied twice as shown in Figure 2, such that the dimension of the composite system becomes $n_c = 16$ and its global relative degree $\{r_1, r_2\} = \{8, 8\}$ is achieved. Therefore the condition $r_1 + r_2 = n_c$ is also fulfilled, so that composite system including auxiliary states ($\xi = [\xi_1, \ldots, \xi_6]^T$ and $\mathbf{z}$, dummy ones) can be transformed into a linear and controllable system in normal coordinates. Noninteracting control with stability is determined with the following control laws

$$u_1 = (-f_6 + \xi_1 - D_{12}u_2)/D_{11} \qquad (3)$$
$$u_2 = (-f_7 + \xi_4 - D_{21}u_1)/D_{22}$$

where the reference inputs $\mathbf{v} = [v_1 \ v_2]^T$ in Figure 2 are designed as

$$v_1 = -800(q_1 - \theta_{1d}) - 60q_6 - \dot{q}_6 \qquad (4)$$
$$v_2 = -800(q_2 - \theta_{2d}) - 60q_7 - \dot{q}_7$$

where the gains are determined by trial and error. In the next section, these controller gains will be optimized. The zero dynamics(ξ and z) of system (2) (basically built by a chain of integrators with appropriate feedback law) is stable at the origin. After applying nonlinear *dynamic* state feedback control laws given by equation 3 and rearranging the state equations, we have the following subsystem

$$\dot{\mathbf{q}} = \tilde{f}(\mathbf{q}, \xi) + [\tilde{g}_1 \quad \tilde{g}_2] \begin{bmatrix} u_1 \\ u_2 \end{bmatrix} \qquad (5)$$

where $\tilde{g}_1 = 0$ and $\tilde{g}_2 = 0$. Besides the actual input torques are applied only to rigid coordinates and affect the equations of $\dot{q}_6$ and $\dot{q}_7$. For the system (5) calculations prove that $[ad_{\tilde{f}} \tilde{g}_1, ad_{\tilde{f}} \tilde{g}_2] = 0$ and in the light of [16, Th. 7.4.4], we have

Lemma 1.1: If $[ad_{\tilde{f}}^k \tilde{g}_1, ad_{\tilde{f}}^h \tilde{g}_2] = 0$ for all $k \geq 0$ and all $h \geq 0$ then the necessary condition for noninteracting control with stability of the system (2) via dynamic feedback is fulfilled.

where $ad_f^k g = [f, ad_f^{k-1} g]$ for $k \geq 1$, $ad_f^0 g = g$ and also $ad_f^1 g = [f, g]$ is the Lie product. Asymptotic stability of the modal coordinates is guaranteed [16, Th. 9.6.2] for its proof see also [17, section 12.3] such that

$$\lim_{t \to \infty} \mathbf{q}(t) = 0$$

which has been verified by simulations in the present study.

B. Error-Feedback Controller for Adaptive Case

Designing an internal-model based control scheme can generate the control law C_σ that renders the output-zeroing manifold invariant that corresponds to placement of transmission zeroes in the transfer function from disturbance to output in linear systems. The internal model part of the controller is augmented with a robust stabilizer as a second part of the controller later on. Based on the set-up and the system (5) in the previous section the controller architecture has been extended to include the adaptive case. The adaptive internal model approach in [7], [18] has been applied in this study, yielding the error and disturbance dynamics as follows

$$
\begin{aligned}
\dot{\mathbf{z}} &= f_0(\mathbf{z}, q_1, q_2, \mathbf{w}, m_2) \\
\dot{q}_1 &= q_6 \\
\dot{q}_2 &= q_7 \\
e_1 &= q_6 \qquad (6)\\
\dot{e}_1 &= \xi_1(v_1) + \rho_1(w_1) \\
e_2 &= q_7 \\
\dot{e}_2 &= \xi_4(v_2) + \rho_2(w_2)
\end{aligned}
$$

where $\mathbf{z} = [q_8 \ q_9 \ q_{10}]^T$, m_2 is the varying tip-mass, v_1, v_2 are the control inputs, $\rho_1(w_1) = w_1$, $\rho_2(w_2) = w_2$ and $\mathbf{w}$ represents *neutrally stable* exosystem or disturbances with the following dynamics :

$$
\begin{aligned}
\dot{\mathbf{w}} &= S \cdot \mathbf{w} \\
S &= \begin{bmatrix} 0 & \sigma \\ -\sigma & 0 \end{bmatrix}
\end{aligned}
$$

where σ is unknown exosystem parameter.After some calculations, the control laws, C_σ, for the nonadaptive internal model are determined as

$$
\begin{aligned}
C1_\sigma &= L_S^2 \, \rho_1(w_1) = -\sigma^2 \cdot w_1 \\
C2_\sigma &= L_S^2 \, \rho_2(w_2) = -\sigma^2 \cdot w_2 \\
L_S^4 \, C_\sigma &= a_0 C_\sigma + a_1 L_S \, C_\sigma + a_2 L_S^2 \, C_\sigma + a_3 L_S^3 \, C_\sigma
\end{aligned}
$$

where all a_i's depend on σ. After solution of the last equation for $a_i(\sigma)$ terms we have the linear observable system for the part of internal model of the controller as follows :

$$
\begin{aligned}
\Phi(\sigma) &= \begin{bmatrix} 0 & 1 & 0 & 0 \\ 0 & 0 & 1 & 0 \\ 0 & 0 & 0 & 1 \\ a_0(\sigma) & a_1(\sigma) & a_2(\sigma) & a_3(\sigma) \end{bmatrix} \\
\Gamma &= (1 \ 0 \ 0 \ 0) \\
\dot{\eta} &= \Phi(\sigma) \cdot \eta \\
u_{im} &= \Gamma \cdot \eta
\end{aligned}
$$

where the spectrum of $\Phi(\sigma)$ must contain the distinct eigenvalues of the exosystem. Higher order harmonics of these sinusoidals may be generated by the nonlinearities of the plant, thus the spectrum of $\Phi(\sigma)$ must as well contain multiples of the eigenvalues of the exosystem [7]. Applying a linear similarity transformation to the above system we have the canonical internal model as follows

$$\dot{\eta} = (F + G\Psi_\sigma) \cdot \eta$$
$$u_{im} = \Psi_\sigma \cdot \eta$$

Since the derivatives of the errors will be used in the controller implementation, the errors and their derivatives should be estimated by a high-speed observer. Then the linear observer can be chosen as

$$\dot{\hat{q}} = M_g \cdot \hat{q} + L_g \cdot e_i \qquad i = 1, 2$$

where

$$M_g = \begin{bmatrix} -g \cdot c_1 & 1 \\ -g^2 \cdot c_0 & 0 \end{bmatrix}$$

$$L_g = \begin{bmatrix} g \cdot c_1 \\ g^2 \cdot c_0 \end{bmatrix}$$

$g > 0$ is a design parameter, and the polynomial $p_c(\lambda) = \lambda^2 + c_1 \cdot \lambda + c_0$ is Hurwitz. In order to prevent the occurrence of finite escape times for large value of the parameter g, the estimates need to be saturated. The controller is then implemented using the estimates instead of the measured states. In order to solve the problem of semi-global robust output regulation for system (6) we need to define $\hat{\vartheta}$ from the estimates to use it in the feedback path of adaptation and stabilization [7, Th. VII.1]. Consider the new dynamic error feedback controller :

$$\hat{\vartheta}_1 = \hat{q}_2 + k\hat{q}_1$$
$$\hat{\vartheta}_2 = \hat{q}_4 + k\hat{q}_3$$
$$\dot{\zeta}_i = (F + G\hat{\Psi}_i)\zeta_i - KG \cdot sat(l, \hat{\vartheta}_i)$$
$$\frac{d}{dt}\hat{\Psi}_i = -\gamma \cdot sat(l, \hat{\vartheta}_i)\zeta_i^T \qquad (Adaptation \quad Rule)$$
$$v_i = \hat{\Psi}_i\zeta_i + v_{si} \quad and \quad i = 1, 2.$$

where the v_{s1}, v_{s2} are as defined below and $sat(\cdot, \cdot)$ is a saturation function defined as

$$sat(l, s) = \begin{cases} s, & |s| \leq l \\ \frac{s}{|s|}, & |s| > l \end{cases}$$

In this paper to stabilize the system v_{si} control inputs given below have been used, different than the approach in [7] such that

$$v_{s1} = -K_{c1}(q_1 - \theta_{1d}) - K_{c2} q_6 - \dot{q}_6$$
$$v_{s2} = -K_{c1}(q_2 - \theta_{2d}) - K_{c2} q_7 - \dot{q}_7$$

where K_{c1} and K_{c2} are optimized by a novel optimization method, an evolutionary algorithm termed as "Big Bang - Big Crunch", BB-BC [19] . This new method relies on one of the theories of the *evolution* of the universe; namely, the Big Bang and Big Crunch Theory. In the Big Bang phase, energy dissipation produces disorder and randomness is the main feature of this phase; whereas, in the Big Crunch phase, randomly distributed particles are drawn into an order. Inspired by this theory, an optimization algorithm is developed in [19]. The algorithm generates gaussian-distributed random points in the Big Bang phase and shrinks those points to a single representative point via a center of mass approach in the Big Crunch phase. Both phases follow each other iteratively with certain constraints. It is shown in [19] that the performance of the new BB-BC method outperforms the classical Genetic Algorithm (GA)for many benchmark test functions.

IV. SIMULATION RESULTS

A. Non-Adaptive Case

The proposed control scheme is tested with the simulation program implemented in MATLAB. The parameters used in the model for system (2) given in [5] are listed in TABLE I.

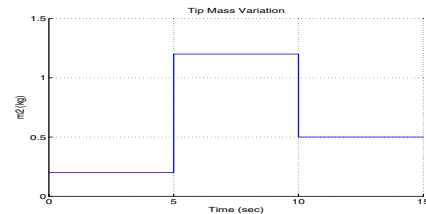| Parameter	Value
Length of links, $L_1 = L_2$	0.5 m
Young's Modulus, E	200 GPa
Density, ρ	7800 kgm^{-3}
Cross-sectional area	$9e - 5$ m^2
Hub inertia, I_0	0.02 kgm^2
Centroidal inertia, $I_1 = I_2$	$4.7e - 11$ m^4
Tip mass, m_2	0.2, 1.2, 0.5 kg
θ_{1d} (desired)	$\pi/2$ rad
θ_{2d} (desired)	$-\pi/2$ rad
Coef. of Viscous fric. V_f	0.001
Coef. of Coulomb fric. C_f	0.07

TABLE I

PARAMETERS OF THE FLEXIBLE ARM.

Fig. 3. Tip Mass Variation

The simulation results are presented in the Figures 3 - 5 and in [14]. Tip-mass has been varied as can be seen in Fig. 3. Non-adaptive case with tip-mass variation is simulated first without any disturbance. No significant changes can be observed in time responses compared to the case of constant tip-mass.This shows the robustness of the proposed controller.The flexible hub-arm system is a non-minimum phase in nature. Therefore,the initial torque
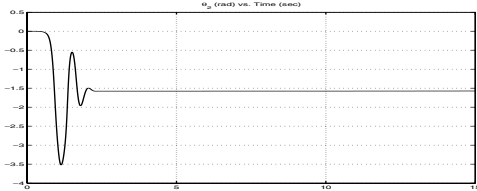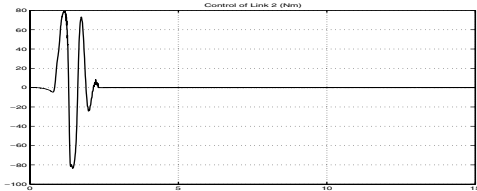
Fig. 4. Θ_2 - Non-Adaptive Case

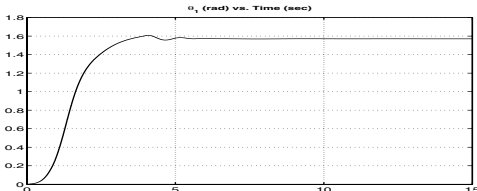Fig. 5. Control on Θ_2 - Non-Adaptive Case

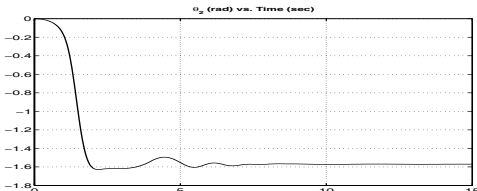Fig. 6. Θ_1 - Adaptive Case 1

Fig. 7. Θ_2 - Adaptive Case 1
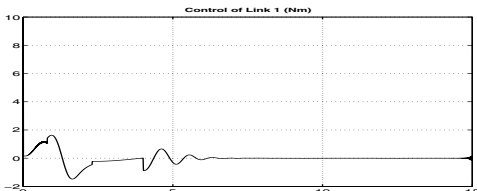
Fig. 8. Control on Θ_1 - Adaptive Case 1
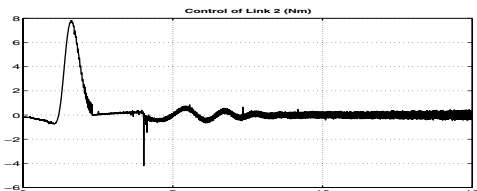
Fig. 9. Control on Θ_2 - Adaptive Case 1
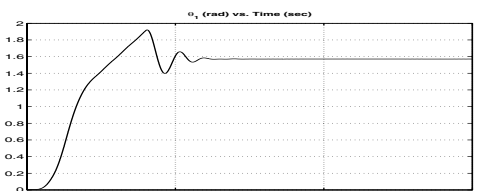
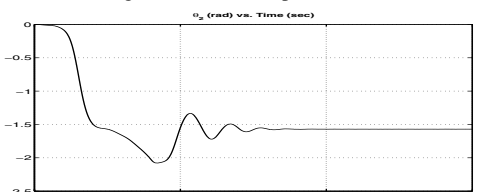Fig. 10. Θ_1 - Adaptive Case 2

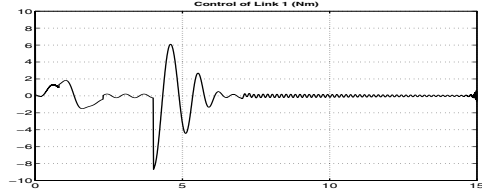Fig. 11. Θ_2 - Adaptive Case 2

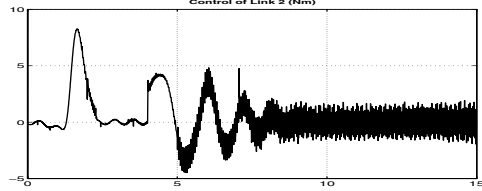Fig. 12. Control on Θ_1 - Adaptive Case 2

Fig. 13. Control on Θ_2 - Adaptive Case 2

may result in undesired vibration at the beginning of the motion, can be seen in Figure 4.

B. Adaptive Case

The parameters used in the model for system (6) are listed in TABLE II.

Parameter	Value
Coef. of Viscous fric. V_f	0.001
Coef. of Coulomb fric. C_f	0.0
σ_0 to initiate Adaptation	1
σ exosystem @ case1	1 and 2 after 7th second
σ exosystem @ case2	10 and 40 after 7th second
$g = 10, \qquad k = 0.5$	$K = 0.001$
$a_0 \qquad$ for $\Phi(\sigma)$	$-100\sigma^4$
$a_2 \qquad$ for $\Phi(\sigma)$	$-101\sigma^2$
$a_1 = a_3 = 0 \quad$ for $\Phi(\sigma)$	$c_0 = 2, \quad c_1 = 3$
$w_1(0)$ exosystem	$\frac{\pi}{20}$
$w_2(0)$ exosystem	$\frac{-\pi}{20}$

TABLE II

ADDITIONAL PARAMETERS FOR THE ADAPTIVE CASES.

The simulation results for two different cases are presented in Figures 6 - 13. In both cases adaptation is turned on after 4 seconds and never turned off later on. In the first case that has low-frequency disturbance,we start with $\sigma = 1$ until $t = 7$ secs and then change to $\sigma = 2$ for the rest of the simulation. Fortunately, possible undesired vibration at the beginning of the motion (especially for link 2) is prevented very well in the first case by optimization of the controller parameters. In the second case that has high-frequency disturbance,we start with $\sigma = 10$ until $t = 7$ secs and then change to $\sigma = 40$ for the rest of the simulation. In particular, $\sigma = 40$ corresponds to lowest resonant frequency of neglected higher modes (first link: 344 rad/sec, second link: 245 rad/sec) of vibration, but the proposed controller is still good for handling high frequency disturbances and also adaptation is quick as well. The adaptive case 1 has much less overshoot (almost none) and more smooth control history compared with the case 2. The canonical parametrization of the internal model has been chosen such that the matrix F is Hurwitz and the triplet (F, G, Ψ_0) has been obtained from

balanced-controllable canonical form. In order to initiate the adaptive update rule Ψ_0 has been calculated by

$$\Phi(\sigma_0) = F + G\Psi_0.$$

In the first part of the simulation in both adaptive cases, initial conditions for the exosystem have been chosen in the $[-\pi/20, \pi/20]$ interval. As can be seen in figures 6 to 9, the adaptation mechanism worked very well. However, in the second part of the simulation initial conditions for the exosystem have been chosen $[-\pi/3, \pi/3]$ interval and as can be seen in [14], it took longer to adapt to disturbances with a significant overshoot compared to the first part, since the domain of attraction in the second part has been expanded largely, and also the amplitude of the external disturbances increased from 0.2 to 1.5. This shows the robustness of the adaptive controller and also the *boundary of basin of attraction* is close to boundary of the interval $[-\pi/3, \pi/3]$.

In both adaptive cases, the controller gains have been optimized by BB-BC [19]. This optimization improved on the results reported in [14]. Comparing figures 4 to 5 which represent the non-optimized and non-adaptive case with figures 6 to 13 which represent the optimized-adaptive cases, is observed that overshoot decreased enormously (almost none at case 1), and total control energy is reduced since the amplitude of the control signal reduces to the one tenth of the values in the non-optimized cases as given in [14].

V. Conclusions

It has been shown by the simulation results that the new design method can provide asymptotic stability of flexural modes and set-point regulation of rigid modes simultaneously. Also, the single nonadaptive controller has robustness with respect to tip mass changes, verified by simulations.

In the adaptive case the size of the domain of attraction for exosystem states is important for fast adaptation and smooth time history.The proposed controller has also robustness with respect to external disturbances, since the controller achieved good performance when the amplitude of sinusoidal increased more than sevenfold of its value . The stabilizer part of the controller with Adaptive Internal Model has been introduced for the first time in this research. The optimization of the stabilizer gains improved the performance significantly.

References

[1] M.W. Vandegrift, F.L. Lewis, and S.Q. Zhu, 'Flexible-Link robot arm control by a feedback linearization/Singular perturbation approach', *Journal of Robotic Systems*, vol. 11(7), pp. 591-603, 1994.

[2] M.R. Rokui and K. Khorasani,'Experimental results on discrete-time nonlinear adaptive tracking control of a Flexible-link Manipulator', *IEEE Transactions on systems, man, and cybernetics*, vol.30/1, pp.151-164, 2000.

[3] B. Siciliano and L. Villani,'Two-Time scale force and position control of flexible manipulators',*Proceedings of the IEEE International Conference on Robotics and Automation*, pp. 2729-2734,Seoul, 2001.

[4] X. Zhang,W. Xu,S.S. Nair,'PDE modeling and control of a flexible two-link manipulator',*Proceedings of the American Control Conference*, pp. 3796-3801,Anchorage, 2002.

[5] Ye Zhu, Jinhao Qiu, Junji Tani,'Simultaneous Optimization of a Two-link Flexible Robot Arm',*Journal of Robotic Systems*, vol. 18(1), pp. 29-38, 2001.

[6] A. Alleyne, and M. Pomykalski,'Control of a Class of Nonlinear Systems subject to Periodic Exogenous Signals',*IEEE Transactions on Control Systems Technology*, vol.8/2, pp.279-287, 2000.

[7] A. Serrani, A. Isidori and L. Marconi,'Semiglobal Nonlinear Output Regulation with Adaptive Internal Model',*IEEE Transactions on Automatic Control*, vol.46/8, pp.1178-1194, 2001.

[8] L. Meirovitch, *Dynamics and Control of Structures*, New York: John Wiley Sons, 1990.

[9] R.J. Theodore,A.Ghosal,'Comparison of the Assumed Modes and Finite Element Models for Flexible Multilink Manipulators',*Int Journal of Robotics Research*, vol. 14/2, pp. 91-111, 1995.

[10] M. Moallem, R.V. Patel, K. Khorasani, *Flexible-link Robot Manipulators:Control Techniques and Structural Design*, London: Springer-Verlag, 2000.

[11] L. Meirovitch, *Fundamentals of Vibrations*, New York: McGraw-Hill, 2001.

[12] J.N. Reddy, *An Introduction to the Finite Element Method*, New York: McGraw-Hill, 1993.

[13] G.G. Hastings and W.J.Book,'A Linear Dynamic Model for Flexible Robotic Manipulators',*IEEE Control System Magazine*, vol.7, pp.61-64, 1987.

[14] M. Dogan, Y. Istefanopulos, E.D. Diktas, 'Nonlinear Control of two-link Flexible Arm with Adaptive Internal Model, *Proc. IEEE International Conference On Mechatronics*, pp. 292-298, Istanbul, 2004.

[15] J.P. Den Hartog, *Mechanical Vibrations*, New York: Dover, 1985.

[16] A. Isidori, *Nonlinear Control Systems, 3rd edition* , New York: Springer-Verlag, 1995.

[17] A. Isidori, *Nonlinear Control Systems II* , London: Springer-Verlag, 1999.

[18] C.I. Byrnes, A. Isidori ,'Limit Sets, Zero Dynamics, and Internal Models in the Problem of Nonlinear Output Regulation',*IEEE Transactions on Automatic Control*, vol.48/10, pp.1712-1723, 2003.

[19] O.K. Erol, I. Eksin, 'A New Optimization Method: Big Bang - Big Crunch ', accepted for publication in *Advances in Engineering Software*, 2005.